

# Restoration of motion blur image for detection robot by Generative Adversarial Network

Jifeng Cui

College of Computer Science and Technology  
Shandong University of science and technology  
266590 Qingdao, Shandong Province, China  
godisabiggirl@163.com

Jin Han

College of Computer Science and Technology  
Shandong University of science and technology  
266590 Qingdao, Shandong Province, China  
\*Correponding Author:shnk123@163.com

Received February 2021; revised April 2021

---

**ABSTRACT.** *The inspection robot is affected by its motion and the ground environment during its operation, and the collected images are prone to motion blur. The traditional algorithm has a large amount of calculation and a long processing time, which cannot meet the real-time needs of detection robots. For this problem, the present work is based on a Generative Adversarial Network. The generator uses a lightweight algorithm combining target detection FPN and depth separable convolution MobileNetV3. The discriminator uses a relative discriminator, and the loss function is composed of four mixed loss functions. Through the experimental verification on the Gopro data set and the actual collected data set, the processing speed of the lightweight algorithm given in the paper reaches 0.05s, which meets the real-time requirements of the inspection robot. It can effectively restore the motion blur images of the inspection robot and the restored images are more detailed and accurate. The lightweight algorithm requires fewer calculations, and the processing speed is faster. It can be directly run in the inspection robot, effectively improving its work efficiency, and has a certain reference value for image restoration of other embedded platforms.*

**Keywords:** Generative Adversarial Network, Fast Image Restoration, Blurred Image, Motion Blur.

---

**1. Introduction.** With the rapid development of computer technology, the application of inspection robots has become more extensive. The working environment and working methods of inspection robots are relatively complicated. Affected by their motion and ground environment, they will shake or vibrate, and there will be relative motion between shooting scenes or objects, and the obtained images are prone to motion blur, which affects the processing results. Therefore, in the process of using the robot, it is particularly important to better restore the motion-blurred image.

**1.1. Traditional algorithm.** Image deblurring solutions can be divided into two categories according to whether the blur kernel is known: non-blind deblurring and blind deblurring. Non-blind deblurring requires a known blur kernel for deblurring, which has some limitations. Therefore, blindly removing motion blur in images is one of the most challenging problems in image processing. In the blind de-motion blur, Krishnan

et al. [1] proposed a blind de-blurring algorithm based on variational Bayes and used the Richardson-Lucy algorithm to restore the image. It is easy to lose the high-frequency information of the image, which reduces the quality of the restored image. And greatly increases the difficulty of subsequent processing on the restored image Hirsch et al. [2] proposed a blind deblurring algorithm that uses a combination of local uniform blur to approximate spatial non-uniform blur, but this method lacks effective modeling of the formation process of motion blur, and the deblurring performance is not good in practical applications. Later, Zhang et al. [3] Based on the Bayesian-inspired penalty function (Bayesian-inspired penalty function), the fuzzy kernel and noise are integrated uniquely. The algorithm can automatically adapt to the quality of the input blurred image. And high-quality images have a greater contribution to the entire estimation process. To better solve the more complex motion blur problem, Cho et al. [4] proposed an algorithm that can estimate multiple blur kernels in the scene, and performs image segmentation, and solves the problem of motion blur by alternately optimizing regularized energy function.

In summary, the traditional deblurring method is based on the physical model of the image imaging process, applying various constraints to simulate the blur characteristics, and achieves image deblurring through mathematical modeling. Traditional methods involve heuristic parameter adjustments and complex calculations, but the blurring in real situations is much more complicated than modeling, so a deblurring method based on neural network learning is proposed.

**1.2. Motion blurred image restoration algorithm based on deep learning.** Zhou et al. [5] used a neural network for image restoration for the first time and proposed an image restoration model based on a discrete Hopfield neural network. Jain et al. [6] used convolutional neural networks for image denoising, proving that convolutional neural networks can directly learn an end-to-end non-linear mapping from low-quality images to clear images, and can better restore images. Chakrabarti et al. [7] proposed a method of blindly removing motion blur in images, predicting the Fourier coefficients of a deconvolution filter through a convolutional neural network, and estimating the motion kernel to restore the blurred image. The effect is good, but it takes a long time. Xu et al. [8] proposed to use a convolutional neural network to learn and extract the edge information of the blurred image to supplement the prior information of the image blur kernel, thereby improving the accuracy of the blur kernel estimation. When the noise is large, the edge extraction ability is reduced, and the estimation of the blur kernel is inaccurate, so the recovery effect is poor. Later, a continuous deblurring method proposed by Sun et al. [9] establishes a non-uniform deconvolution model to deblur the image, which is only suitable for certain types of blur. Nah et al. [10] and Noroozi et al. [11] uses a convolutional neural network to directly generate a deblurred image end-to-end. This method inputs the blurred image into the network model during testing, and the output is the deblurred image. To further improve the effect, Kupyn et al. [12] proposed DeblurGAN to remove the image motion blur model, which directly restores the clear image in an end-to-end manner, and uses multiple sets of loss functions to optimize the network. Increase the stability of the confrontation generation network, so that the restored image has more texture information. At the same time, the real-time performance is improved by 5 times.

At present, there is little deep learning research on the motion blur images of inspection robots. With the development of science and technology, inspection robots are used more widely, and the pictures taken when inspection robots are running are prone to motion blur. Therefore, the enhancement of motion-blurred images has important value. In order to improve the effect of image deblurring, this paper adopts an image deblurring model based on generative adversarial network. The model adopts the combination of

the FPN of target detection and the deep separable convolution MobileNetV3 to better utilize the semantic information of low-level features and the semantic information of high-level features, and accelerate the network convergence speed. At the same time, the relative discriminator is used to enrich the details of the restored image. Through the confrontation training between the generative network and the discriminant network, the generative network is finally used to generate clear images end-to-end.

**2. Characteristics and Analysis of Blur Image of Inspection Robot.** Restoring the motion blur generated by the inspection robot can be regarded as a special image-to-image translation process. Affected by the working mode and working environment of the inspection robot, its blur has the characteristics of large scale, multiple angles, and more noise. Traditional algorithms need to know the fuzzy kernel to restore blurred images, and the adversarial generation network can restore motion-blurred images end-to-end through the game between the generator and the discriminator.

**2.1. Motion blur.** During the operation of the inspection robot, the motion blur can be expressed by the following formula:

$$I = L * B + R \quad (1)$$

Among them,  $L$  is the fuzzy kernel, which is related to the trajectory of the inspection robot and the rotation angle of the camera (the mathematical model is recorded as  $I$ ),  $B$  is the clear image to be obtained, indicates the convolution operation, and  $R$  is the work environment Noise, the final output  $I$  is a blurred image, which is a blurred image taken by the inspection robot. The restoration of the blurred image taken by the inspection robot is the reverse process of the above formula. That is, the content of this article is the process of solving  $B$  when  $I$  is known. Therefore, motion blur can also be regarded as a special image-to-image translation task [12].

When the inspection robot takes pictures, it is affected by its working environment and its own motion. During the exposure period, there is relative motion between the shooting scene or the shooting object. The principle of motion blur is shown in FIGURE 1:

The inspection robot takes images when it moves from point  $P$  to point  $Q$ , and point  $C$  is the target object on the ground. The robot takes a picture at point  $P$  and exposes it. In theory, the imaging of point  $C$  is point  $A$  at this time. Since the robot moves to point  $Q$  at the end of the exposure, the imaging point  $C$  at point  $Q$  is point  $B$  ( $a$  is the corresponding point of point  $A$  in the figure), resulting in motion blur. During the operation of the inspection robot, the motion blur kernel generated is complex and random. Therefore, the traditional restoration method that needs to estimate the fuzzy kernel is not suitable for this scenario.

**2.2. Analysis of the production and restoration method of the motion blur of the inspection robot.** The working environment of the inspection robot is complex, and the types of motion blur are also diverse. The traditional methods commonly used to deal with its blur include Wiener filtering and inverse filtering.

**2.2.1. Characteristics of motion blur of inspection robot.** The working mode and working environment of the inspection robot determine that the images taken by it have the following characteristics:

- (1) When the inspection robot is working, it is often in a high-speed motion state, and it is easy to produce blurred pictures with a large motion blur scale.
- (2) Affected by factors such as light, fog, and dust in the working environment, the captured image contains uncertain noise and affects the deblurring effect.

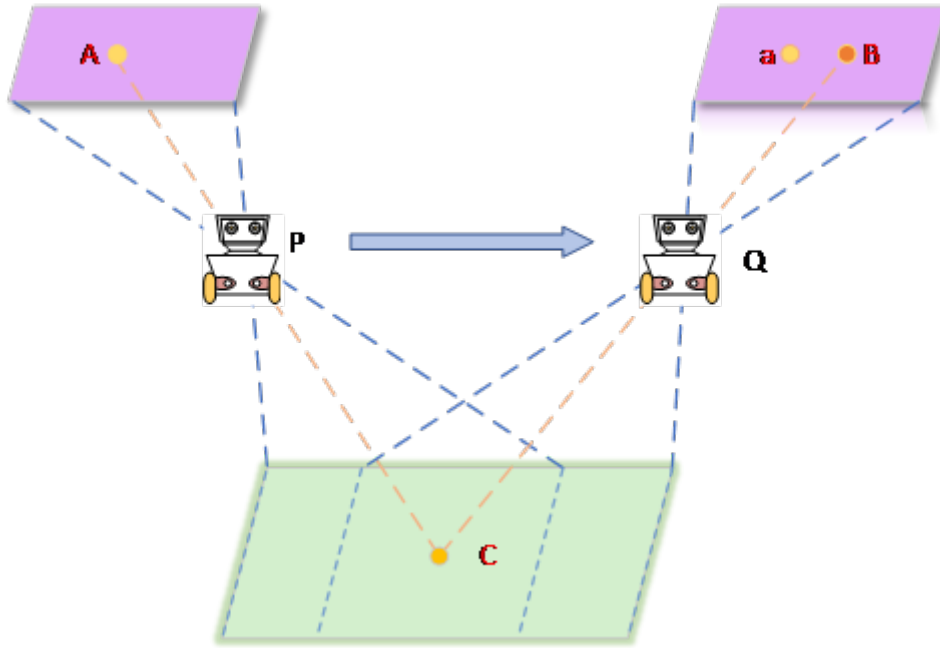


FIGURE 1. Schematic diagram of the motion blur of the inspector robot

(3) The work scene of the inspection robot is complex, which may include objects such as instruments, meters, crowds, buildings, and vehicles. And there are many types of targets in the image.

(4) The inspection robot is affected by the working environment and terrain and has various motion modes, including uniform motion, acceleration and deceleration motion, circular motion, sine and cosine motion, etc. Different motion methods produce blurred images with their characteristics.

*2.2.2. Analysis of restoration method for motion blur of inspection robot.* Traditional non-blind deblurring algorithms, Wiener filtering and inverse filtering, require known fuzzy kernels. Although it is currently possible to estimate the blur kernel based on the movement of the inspection robot, obtain the current speed, camera deflection parameters, etc. But it takes too long to obtain the data and analyze it to estimate the blur kernel. And the effect is not good for noisy pictures. The restored image is prone to distortion and artifacts. Therefore, the traditional algorithm in practice takes a long time to restore the motion blur generated by the cruise robot, which has poor noise resistance. The restored image is easily distorted and it is not suitable for restoring its motion-blurred pictures. The Generative adversarial network is composed of generators and discriminators. Through mutual game confrontation training, it can better restore motion-blurred pictures. It is also one of the most promising methods for unsupervised learning in recent years.

**2.3. Generative adversarial network.** The generative adversarial network (GAN) is a generative model designed by Goodfellow et al. [13] in 2014. The learning goal is achieved through the mutual game process of the generator and the discriminator. It is widely used in image and voice fields [14]. The structure diagram of the fuzzy map restored by the generative adversarial network model is shown in the figure above: the generative countermeasure network is composed of a generator and a discriminator. The generator receives a fuzzy image and then generates a corresponding example. The discriminator will receive the samples generated by the generator and the samples from real samples

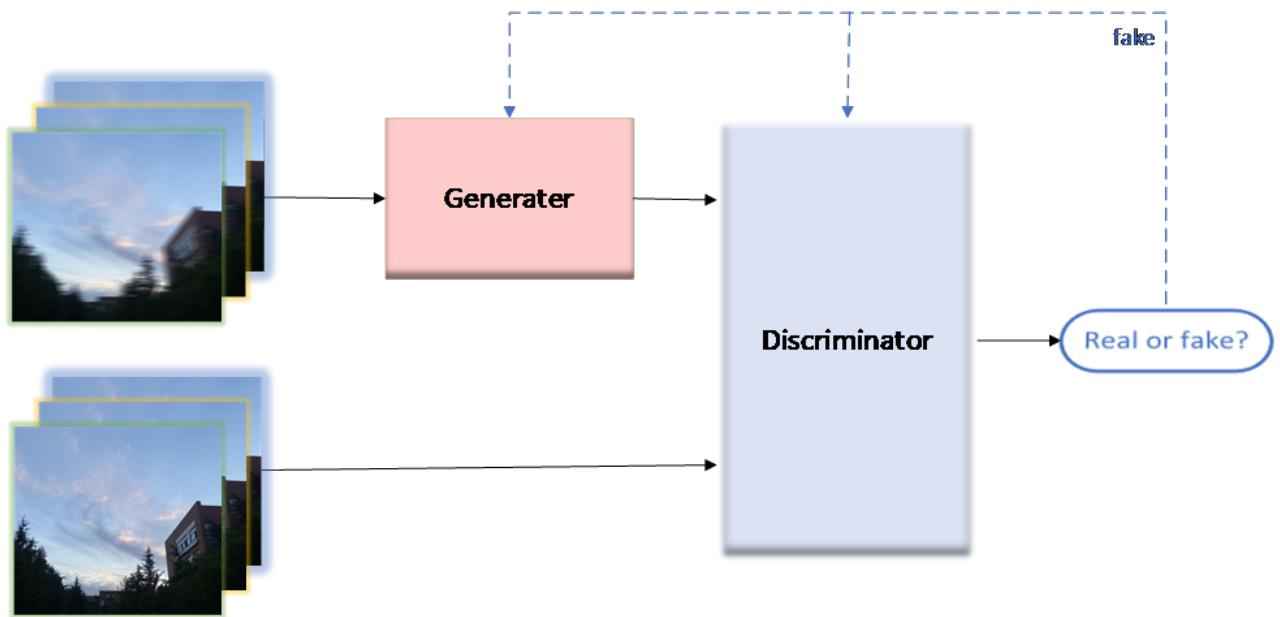


FIGURE 2. Schematic diagram of confrontation generation network

and judge the authenticity of the samples. The generator continues to strengthen its ability to make the generated sample closer and closer to the real sample, that is, the discriminator is increasingly unable to distinguish whether the sample is real. Through continuous iteration of the above process, until the discriminator is not clear whether the received sample is from a real sample or a generated sample. The generation network and the discriminant network use the loss function for confrontation training. The purpose of network confrontation training is to make the image generated by the generator closer to the real data distribution. After continuous confrontation training and iterative optimization, when the discriminant network finally cannot discriminate the true and false data, it is considered that the generating network has learned the true data distribution.

**3. Algorithm Description.** The algorithm in this paper uses a generative adversarial network, and the generator uses FPN and MobileNetV3, the discriminator uses a relative discriminator, and the generator and the discriminator are trained against each other to obtain better deblurring results.

**3.1. Generator.** Most of the generators of the traditional generative adversarial network use CNN networks, which deal with different levels of blur at different scales, which requires a large amount of calculation, and it is difficult to effectively extract the features of each layer. The algorithm given in this paper combines the FPN of target detection and the lightweight MobileNetV3, which reduces the amount of calculation and extracts semantic information of different layers and merges the features of these different layers to achieve a better image restoration effect.

The traditional image deblurring network is usually a ResNet-type structure. It uses multi-stream CNN to process different levels of blur at different scales, which is often time-consuming and labor-intensive. Most algorithms use multi-scale feature fusion [15], to process images to obtain better results. And use high-resolution images to solve practical problems in the field of Internet of Things [16]. FPN [17] (Feature Pyramid Network) uses the semantic information of low-level features and the semantic information of high-level features at the same time. It can obtain rich semantic information by extracting features

at different levels and fusing them to obtain better results. The FPN algorithm was originally designed to be applied to target detection. It can generate multiple different levels of feature mapping layers from the upper and lower path directions and extract deeper and richer semantic information. At the same time, the horizontal connection merges the feature maps of the same size in the two paths to enhance the extracted high-resolution features. The feature pyramid network is used to obtain strong semantic information by extracting feature maps of different scales, which is of great significance for the generator to generate images with rich details. Orest et al. [18] introduced the idea of the feature pyramid network to image deblurring for the first time and achieved very good results. In this paper, FPN is used to fuse the features of different layers to obtain five feature maps of different proportions. The upper and lower paths and their horizontal connections can effectively extract the rich semantic information of different layers. The final feature map is upsampled to the same size, to restore and reconstruct the blurred image.

The generator of this article uses MobileNetV3-Large [19] as the backbone network. Bneck is a unique structure of MobileNetV3. It combines the inverse residual structure of MobileNetV2 [20] with a linear bottleneck and the deep separable convolution of MobileNetV1 [21]. It uses h-swish instead of swish function, which reduces the amount of calculation and is more lightweight. The formula is as follows:

$$h - swish[x] = x \frac{RELU6(x + 3)}{6} \quad (2)$$

For embedded platforms, sigmoid will consume more computing resources. Using h-swish as the activation function can reduce the amount of calculation, so MobileNet-V3 uses a function to approximate swish.

**3.2. Relativistic discriminator.** In the standard generative confrontation network, the discriminator is used to estimate the probability that the input data is a real sample, and the generator is used to increase the probability that the data is false. It is proposed by Alexia et al. [22] that the probability that real data looks true should be reduced. To minimize the GAN approach divergence, and generate reasonable predictions based on the prior knowledge that half of the small batch of samples are false, the relative discriminator is very necessary. GANs with relative discriminators are more stable and produce higher quality data. The objective function of LSGAN is as follows:

$$\min_D V(D) = \frac{1}{2} E_{x \sim P_{data}(x)} [(D(x) - 1)^2] + \frac{1}{2} E_{z \sim P_z(z)} [D(G(z))^2] \quad (3)$$

$$\min_D V(G) = \frac{1}{2} E_{z \sim P_z(z)} [(D(G(z)) - 1)^2] \quad (4)$$

Orest et al. [18] optimizes and proposes RaGAN-LS loss on the basis of LSGAN, making it more suitable for image restoration. The formula of RaGAN-LS loss is as follows:

$$L_D^{RaLSGAN} = E_{x \sim p_{data}(x)} [(D(x) - E_{z \sim p_z(z)} D(G(z)) - 1)^2] + E_{z \sim p_z(z)} [(D(G(z)) - E_{x \sim p_{data}(x)} D(x) + 1)^2] \quad (5)$$

The adopted RaGAN-LS loss can significantly improve the training speed and stability, so that the restoration results have clearer texture characteristics.

The loss function is composed [23] of four mixed loss functions: adversarial loss function, pixel loss function, feature perception loss function, global and local discriminator loss. The formula is as follows:

$$L_G = \alpha L_a + \beta L_p + \chi L_f + \delta L_{adv} \quad (6)$$

**4. Experimental Results and Analysis.** The experiments in this article are all carried out on a self-made mixed data set, and evaluated on the objective evaluation indicators PSNR and SSIM.

**4.1. Dataset.** Since there are fewer fuzzy image databases for the cruise robot, in order to achieve a better training model effect, the training set is simulated by part of the images in the GoPro dataset and the data set obtained by the network and the pictures taken by the inspection robot. There are a total of 5000 pairs in the data set, and each pair of pictures contains a fuzzy image and a corresponding clear image. The data set contains the scenes that may be photographed during the operation of the inspection robot. Among them, 4000 pairs are used as the training set, and the remaining 1000 pairs are used as the test set.

**4.2. Training details.** The experiment was performed on the data set mentioned above, and the code was written with the pytorch framework to complete the experiment. The experiment was performed on a computer with a processor I7-7700HQ and a GTX1050K GPU graphics card. The initial learning rate of the generator and the discriminator is set to the learning rate of 10-4, which is reduced to 10-8 per 100 iteration. After many training adjustments, set the parameter to  $\alpha = 0.002$ ,  $\beta = 0.5$ ,  $\gamma = 0.006$ ,  $\delta = 0.01$ . The optimizer of the training generator and the discriminator is the Adam optimizer [24] using the training set mentioned above for training, every 4 pairs is a training, and the maximum number of iterations is set to 200. When the number of iterations reaches 150, the loss function tends to be flat, The loss function converges, and the model effect is optimal.

<p>Initialization:  Use stochastic gradient descent algorithm for training, batchsize=4  For k:=1 to (number of training iterations)/10 do    For i:=1 to 5 do      Input a clear image, train the discriminator      Calculate the loss function of the discriminant network      Adam updates the parameters of the discriminator    Save the parameters of the discriminator    For j:=1 to 5 do      Input the blurred image and train the generator      Calculate the loss function of the discriminant network      Adam updates the parameters of the discriminant network    Save generator parameters</p>
---

**4.3. Ablation Study.** Set up a set of comparison experiments to compare with the algorithm used for the cruise robot. The original algorithm uses the generator restnet, the discriminator is WGAN-GP, and the loss function is to generate confrontation loss, content loss and texture loss (Represented by L1 in the table, and our loss function is represented by L2). The scheme used in this article is compared with the original algorithm on a self-made data set. The data obtained is shown in the following table (without special instructions, the experiments in this article are all carried out on the dataset):

TABLE 1. Comparison table of ablation experiments.

Restnet-v2	✓				
WGAN-GP	✓	✓			
L1	✓	✓	✓		
MobileNetV3		✓	✓	✓	✓
FPN					✓
L2				✓	✓
RaGAN-LS loss			✓	✓	✓
PSNR	28.36	28.17	28.19	28.31	28.86
SSIM	0.924	0.905	0.920	0.923	0.928

As can be seen from the above table, our improvements to the original algorithm can gradually improve the performance of the algorithm. In order to illustrate the impact of the lightweight backbone network on the speed of the model, we set up the following experiments.

TABLE 2. Comparison table of backbone network experiments.

	RestNetV2+FPN+RaGAN-LS loss	MobileNetV3+FPN+RaGAN-LS loss
PSNR	28.92	28.86
SSIM	0.930	0.928
Time	0.93s	0.05s

Replacing the backbone network RestNetV2 with MobileNetV3 can significantly increase the speed on the basis of almost unchanged accuracy.

**4.4. Comparative Experiment.** The algorithm in this article is compared with the SRN and deblurgan algorithms, the performance on the objective evaluation indicators and comparison of experimental results as flows:

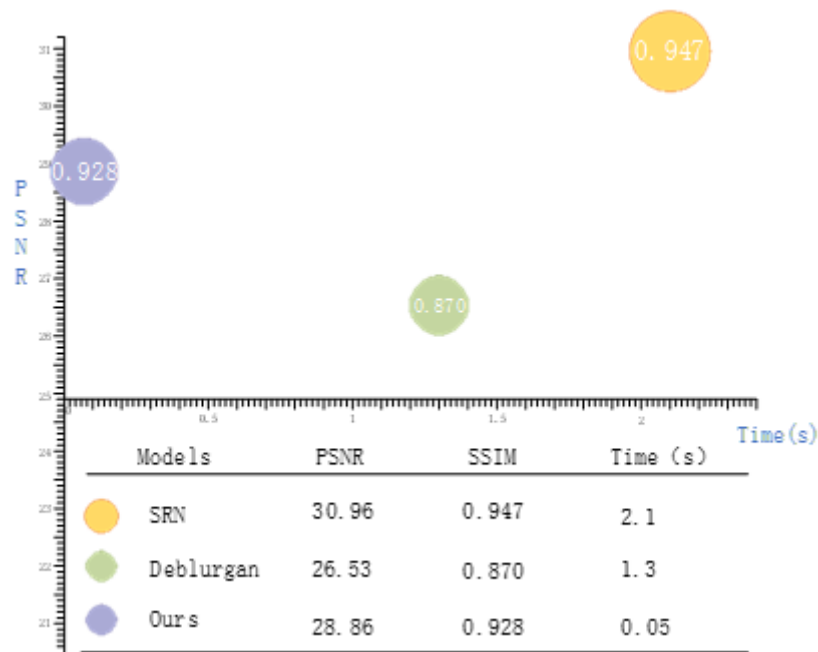


FIGURE 3. The performance on the objective evaluation indicators





FIGURE 4. Comparison table of experimental results

From the perspective of objective evaluation indicators, SRN performs better than other algorithms on objective evaluation indicators SSIM and PSNR, but it takes a long time. The image restored by the deblurgan algorithm has artifacts and so on. Because the algorithm selected in this paper uses MobileNetV3 as the backbone network, it has a small number of layers, so it does not have the best performance on PSNR. From the intuitive point of view of human eyes, the edge information of the restored image obtained by the method in this paper is better restored, the image texture is richer, and there is no ringing phenomenon, and the time-consuming is 0.05, which basically meets the real-time requirements of the inspection robot.

**5. Conclusion.** Aiming at the fuzzy images generated during the operation of the cruising robot, this algorithm is based on generative adversarial network(GAN). The algorithm used combines the advantages of MobileNetV3 and FPN, reducing the amount of calculation while extracting the semantics of the underlying network and the advanced network to improve the accuracy of the algorithm. Both the data set actually collected by the robot and the public data set have good restoration effects. Compared with traditional algorithms and other deep learning algorithms, in terms of objective evaluation indicators, SSIM is 0.928, PSNR is 28.86, and the image processing speed is 0.05s. It can meet the real-time requirements of the cruise robot, and the quality and details of the generated images have certain advantages. In the model structure, the network can be

further optimized. The image processing speed can be accelerated, to have better real-time performance, and the work efficiency of the inspection robot in real-time processing of restoration of blurred images can be further improved.

**Acknowledgment.** This research was supported by Collaborative Education Project of Ministry of Education (201901055015), Postgraduate Education Quality Improvement Project of Educational Commission of Shandong Province of China (ADYAL17034), Excellent Teaching Team Support Project of Shandong University of Science and Technology (JXTD20170503), and Key Project of Natural Science Foundation of Shandong Province of China (ZR2020KE023).

## REFERENCES

- [1] D. Krishnan, and R. Fergus, Fast image deconvolution using hyper-Laplacian priors, *Advances in neural information processing systems*, pp. 1033-1041, 2009.
- [2] M. Hirsch, S. Sra, B. Schölkopf, Spemannstrae, and Germany, Efficient filter flow for space-variant multiframe blind deconvolution, *2010 IEEE Computer Society Conference on Computer Vision and Pattern Recognition*, pp. 607-614, 2010.
- [3] H. Zhang, D. Wipf and Y. Zhang, Multi-image blind deblurring using a coupled adaptive sparse prior, *Proceedings of the IEEE Conference on Computer Vision and Pattern Recognition*, pp. 1051-1058, 2013.
- [4] S. Cho, Y. Matsushita, and S. Lee, Removing non-uniform motion blur from images, *2007 IEEE 11th International Conference on Computer Vision*. pp.1-8.2007:
- [5] Y. -T. Zhou, R. Chellappa, A. Vaid, and K. B Jenkins, Image restoration using a neural network, *IEEE transactions on acoustics, speech, and signal processing*, vol. 36, no. 7, pp. 1141-1151, 1988.
- [6] V. JAIN and S.SEUNG, Natural image denoising with convolutional networks, *Advances in neural information processing systems*, pp. 769-776, 2009.
- [7] A. Chakrabarti, A Neural Approach to Blind Motion Deblurring, *European Conference on Computer Vision. Amsterdam, Netherlands Springer*, pp. 221-235, 2016.
- [8] X.Y. Xu, J.S. Pan, Y.J. Zhang and M.H. Yang, Motion Blur Kernel Estimation via Deep Learning, *IEEE Transactions on Image Processing*, vol. 27, no. 1, pp. 194-205, 2018.
- [9] J. Sun, W. Cao, Z. Xu, and J. Ponce, Learning a convolutional neural network for non-uniform motion blur removal, *The IEEE Conference on Computer Vision and Pattern Recognition(CVPR)*, pp. 769-777, 2015:
- [10] S. Nah, T.H. Kim, and K.M. Lee, Deep multi-scale convolutional neural network for dynamic scene deblurring, *The IEEE Conference on Computer Vision and Pattern Recognition(CVPR)*, pp. 3883-3891, 2017.
- [11] M. Noroozi, P. Chandramouli, and P. Favaro, Motion deblurring in the wild, Roth V, Vetter T. *German conference on pattern recognition (GCPR)*, pp. 65-77, 2017.
- [12] O. Kupyn, V. Budzan, M. Mykhailych, D. Mishkin, and J. Matas, DeblurGAN: Blind Motion Deblurring Using Conditional Adversarial Networks, *In Proceedings of the IEEE Conference on Computer Vision and Pattern Recognition*, pp. 8183-8192, 2018.
- [13] I.J. Goodfellow, J. Pouget-Abadie, M. Mirza, X. Bing and Y. Bengio, Generative adversarial nets, *International Conference on Neural Information Processing Systems*, MIT Press, pp. 2672-2680, 2014.
- [14] Y.L. Wang, H.L. Wu, H.B. Ma, Q.T. Ma, and Q. Ding, Speech Denoising Method Based on Improved Least Squares GAN, *Journal of Network Intelligence*, Vol. 5, No. 3, pp. 113-121, 2020.
- [15] E.K Wang, C.M Chen, M.M Hassan, A. Almogren, "A deep learning based medical image segmentation technique in Internet-of-Medical-Things domain", *Future Generation Computer Systems*, vol. 108, pp. 135-144, 2020.
- [16] E.K. Wang, F. Wang, S. Kumari, J.H. Yeh, and C.M. Chen, Intelligent monitor for typhoon in IoT system of smart city, *The Journal of Supercomputing*, vol.77, no. 3, pp.3024-3043, 2021.
- [17] T.-Y. Lin, P. Dollár, R. Girshick, K. He, B. Hariharan, and S. Belongie, Feature Pyramid Networks for Object Detection, *Proceedings of 2017 IEEE Conference on Computer Vision and Pattern Recognition(CVPR)*, pp. 2117-2125, 2017.
- [18] O. Kupyn, T. Martyniuk, J. Wu, and Z.Y. Wang, DeblurGAN-v2: Deblurring (Orders-of-Magnitude) Faster and Better, *International Conference on Computer Vision(ICCV)*, 2019.

- [19] A. Howard, M. Sandler, G. Chu, L.C. Chen, B. Chen, M. Tan, W. Wang, Y. Zhu, R. Pang, and V. Vasudevan, *Searching for MobileNetV3*, *2019 IEEE/CVF International Conference on Computer Vision (ICCV)*, <https://arxiv.org/abs/1905.02244>, 2020.
- [20] M. Sandler, A. Howard, M. Zhu, A. Zhmoginov, and L-C Chen, *MobileNetV2: Inverted Residuals and Linear Bottlenecks*, *2018 IEEE/CVF Conference on Computer Vision and Pattern Recognition (CVPR)*, <https://arxiv.org/pdf/1801.04381.pdf>, 2018.
- [21] A.G. Howard, M. Zhu, B. Chen, D. Kalenichenko, W. Wang, T. Weyand, M. Andreetto, and H. Adam, *MobileNets: Efficient Convolutional Neural Networks for Mobile Vision Applications*, *Computer Vision and Pattern Recognition*, <https://arxiv.org/abs/1704.04861v1>, 2017.
- [22] A. Jolicoeur-Martineau, *The relativistic discriminator: a key element missing from standard GAN*, *International Conference on Learning Representations (ICLR)*, <https://arxiv.org/abs/1807.00734v3>, 2018.
- [23] A. Alsaiani, R. Rustagi, A. Alhakamy, M.M. Thomas, and A.G Forbes, *Image denoising using a generative adversarial network*, *Proceedings of the 2019 IEEE 2nd International Conference on Information and Computer Technologies*, pp. 126-132, 2019.
- [24] D.P. Kingma, J. Ba, *Adam : a method for stochastic optimization*, *Computer Science*, <https://arxiv.org/abs/1412.6980>, 2017.